Check for updates

Issues and challenges of Fischer–Tropsch synthesis catalysts

Muhammad Amin[1], Muhammad Usman[2], Tatinaidu Kella[3], Wasim Ullah Khan[3], Imtiaz Afzal Khan[4] and Kang Hoon Lee[5]*

[1]Interdisciplinary Research Centre for Hydrogen Technologies and Carbon Management (IRC-HTCM), King Fahd University of Petroleum and Minerals (KFUPM), Dhahran, Saudi Arabia, [2]Chemical and Materials Engineering Department, Faculty of Engineering, King Abdulaziz University, Jeddah, Saudi Arabia, [3]Interdisciplinary Research Center for Refining and Advanced Chemicals, King Fahd University of Petroleum and Minerals, Dhahran, Saudi Arabia, [4]Interdisciplinary Research Center for Membranes and Water Security, King Fahd University of Petroleum and Minerals (KFUPM), Dhahran, Saudi Arabia, [5]Department of Energy and Environmental Engineering, The Catholic University of Korea, Bucheon-si, Republic of Korea

Depletion of oil and gas resources is a major concern for researchers and the global community. Researchers are trying to develop a way to overcome these issues using the Fischer–Tropsch synthesis (FTS) process. The FTS reaction converts a mixture of hydrogen and carbon monoxide gases into a liquid fuel. The reactions are performed in the reactor and in the presence of a catalyst. A series of catalysts, such as iron, cobalt, nickel, and ruthenium, have been used for the FTS process. In iron-based catalysts, the Fe_5C phase is the active phase that produces C_{5+} hydrocarbons. At higher conversion rates, the presence of water in the products is a problem for cobalt catalysts because it can trigger catalyst deactivation mechanisms. Ni-based catalysts play key roles as base catalysts, promoters, and photothermal catalysts in FTS reactions to produce different useful hydrocarbons. Ruthenium catalysts offer not only high activity but also selectivity toward long-chain hydrocarbons. Moreover, depending on the Ru particle size and interaction with the oxide support, the catalyst properties can be tuned to enhance the catalytic activity during FTS. The detailed reaction pathways based on catalyst properties are explained in this article. This review article describes the issues and challenges associated with catalysts used for the FTS process.

1 Introduction

Energy consumption is rapidly increasing due to industrialization. Fuel is essential for industrial applications. Renewable and non-renewable energy sources are the two major sources of fuel (Amin et al., 2022b). Renewable energy sources have a lower environmental impact than non-renewable energy sources. However, renewable energy sources, such as solar, wind, hydro, and nuclear energy, contribute only 19% of the world's energy production. The remaining 81% of energy production comes from non-renewable sources, such as oil, gas, and coal (Bice, 2023). Oil and gas resources are rapidly depleting, which is why researchers have been working on converting coal into hydrocarbon products (Shah et al., 2023). Coal is a major source of syngas (a mixture of hydrogen and carbon monoxide).

Fischer–Tropsch synthesis (FTS) is a process that converts syngas into useful hydrocarbon products. The syngas reaction is carried out in the presence of a catalyst in the reactor (Adnan et al., 2021). A series of reactors, including fixed-bed reactors, slurry bubble columns, tubular reactors, and fluidized bed reactors, were used for the FTS process. Many research articles have been published on FTS catalytic systems using different transition metal catalysts based on the targeted products. In addition, a series of catalysts, such as iron, cobalt, nickel, and ruthenium, have been used for FTS for a long time (Liu et al., 2022; Amin et al., 2024). Among all metals, iron, cobalt, nickel, and ruthenium exhibited adequate activity in the conversion of syngas to hydrocarbons and oxygenates, attributed to their higher hydrogenation activity (Torres Galvis and De Jong, 2013). First-row transition metals, e.g., Fe, Co, and Ni, can operate as a source or sink for electrons, as well as exchange electrons with other species, exist in multiple oxidation states, and undergo redox reactions (Edla et al., 2016; Zhou and Zhou, 2016; Popat et al., 2019). Therefore, compounds of these transition metals are used as catalysts in FTS.

Iron-based catalysts are cost-effective and offer flexible product selectivity. However, they are highly active in the water–gas shift (WGS) reactions. They are commonly utilized at low H_2/CO ratios and are susceptible to carbon deposition and deactivation at high reaction temperatures. Cobalt-based catalysts, particularly metal-oxide-supported cobalt catalysts, have gained significant interest because of their exceptional intrinsic activity, high chain-growth probability, and low activity toward the WGS reaction (Gupta et al., 2023). The features of Co-based materials depend on their geometrical morphology, surface composition, and metal–support interaction (MSI). At higher conversion rates, the presence of water in the products is a problem for cobalt catalysts because it can trigger catalyst deactivation mechanisms. Hydrothermal sintering, the oxidation of cobalt metal to cobalt oxide, and the presence of irremediable cobalt-support compounds are some of these mechanisms (Van de Loosdrecht et al., 2013). Other important considerations include the size of the cobalt nanoparticles, support material, and catalyst synthesis process. Nickel is the fourth most abundant transition metal on the Earth and one of the most frequently utilized elements in metal-based catalysts. Ni is more active in hydrogenation and reforming reactions (De et al., 2016). Nobel Laureate Paul Sabatier described Ni catalysts as "Ni can do all kinds of work and maintains its activity for longer periods" by changing catalyst preparation conditions (Enger and Holmen, 2012a). Ni-based heterogeneous catalysts have been used for CO and CO_2 hydrogenation processes (Usman et al., 2024). Particularly in FTS, Ni catalysts play a vital role in producing different ranges of hydrocarbons and oxygenates, and their performance depends on the Ni nanoparticle size, morphological optimization, and exploration of novel bimetallic combinations on suitable supports. Among FTS catalysts other than transition metals, ruthenium-based catalysts have shown promising activity, higher stability, and a lower extent of deactivation (Abbasi et al., 2019; Badoga et al., 2020). The high activity performance of these catalysts facilitates FTS operation at relatively lower temperatures compared to other types of catalysts (~180°C) (Davis, 2009; Jiang et al., 2017a; Chun et al., 2020; Chen et al., 2022).

Every catalyst has its own advantages and disadvantages in the FTS. In this review, we discuss the issues and challenges of Fe-, Ni-, Co-, and Ru-based catalysts used for the FTS process.

2 Fe-based catalysts for FTS

Iron catalysts have been used in the FTS process because they provide high activity and olefin selectivity. Furthermore, iron catalysts are classified into bulk and supported catalysts. In recent years, research interests have shifted from bulk to supported iron catalysts. The supported iron catalysts have plenty of advantages, such as proper iron dispersion on the surface of the catalyst, high mechanical resistance, higher surface area, and more effective use of the active phase and promoter. The catalytic performance of iron-based catalysts can be enhanced by adding the promoter. A series of promoters such as K, Sb, Au, and Ag have been used for iron-supported catalysts. The potassium promoter has a great impact on hydrocarbon production in terms of selectivity. However, some of the promoters or the presence of a small amount of sulfur or sodium in the catalyst could shift the selectivity toward short-chain hydrocarbon production (C_2–C_4) (Chernyak et al., 2020; Di et al., 2020; Nanduri and Mills, 2020; Li et al., 2021a; Lu et al., 2021b).

The researchers improved the catalytic performance of iron-based catalysts by adding porous support or structural promoters such as SiO_2, TiO_2, Al_2O_3, and ZnO. These supports help increase the dispersion of iron particles and reduce the deactivation rate. In addition, the formation of mixed oxides such as Fe-silicate titanates is hardly reducible and non-active for FTS. The adsorption behavior of FTS products can be changed with the modification of the hydrophobic or hydrophilic properties of catalysts. In recent research, some of the researchers used perfluorodecyltriethoxysilane (PFTS) as an amphiphobic material that improves the stability of the catalyst (Fu et al., 2021; Krzyszczak et al., 2021; Lu et al., 2021a; Ma et al., 2021b; Song et al., 2021; Amin et al., 2022a; Nayak et al., 2022). Figure 1 shows the mechanism of iron-based FTS catalysts.

2.1 Major challenges

Fe-based catalysts are considered cheap as compared to other FTS catalysts, with a comparable syngas production rate (Amin et al., 2022a). Syngas from biomass contains H_2S, HCl, and volatile metals. The purity of syngas is critical since a lack of purity has a detrimental impact on the reactivity. It reacts with Fe at high temperatures, producing FeS and $FeCl_3$. The production of FeS results in catalyst poisoning in a reactor. The formation of the $FeCl_3$ blocks the pores of the catalyst, which reduces the surface area of the catalyst. The lower surface area reduces the activity of the catalyst (Einemann et al., 2024). Mainly, in an iron-containing catalyst, the Fe_5C_2 phase is more active than the Fe_3C phase (Ma et al., 2021b). The stability of the iron-based catalyst is sensitive due to the facet of iron carbides. Mechanistic investigations reveal that the increased FTS activity of {202} χ-Fe_5C_2 surfaces is due to hydrogen-assisted CO dissociation, which decreases the activation energy relative to direct CO dissociation over {112} surfaces. The synthesis of uniformly exposed surfaces on χ-Fe_5C_2 nanocrystals remains a difficult task due to the poor symmetry of the lattice structure (Wu et al., 2024).

Various kinds of support materials such as SiO_2, zeolites, activated carbons, and carbon nanotubes have been used for the
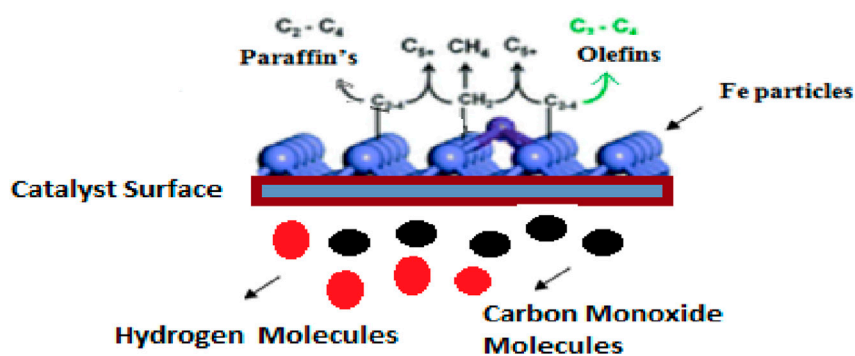
FIGURE 1
Mechanism of iron-based FTS catalysts.

dispersion of Fe particles to increase the exposed metal sites for catalytic reaction (Yahyazadeh et al., 2022). However, for the formation of an active iron carbide phase, the surface of the carbon-based support catalyst needs to be modified. The modification leads to a tunable interaction between iron oxides and supports (Chen et al., 2021).

In order to promote the catalytic activity, Fe is often promoted with alkali metals. It provides a higher number of olefins, and a lower amount of methane is formed. Various kinds of promoters, such as K, Ce, Si, and Cu, have been used for the FTS process (Nie et al., 2019). The potassium promoter stabilized the iron carbide formation during the CO_2 hydrogenation process, which enhanced the C_{5+} production (Martinelli et al., 2020a). However, addition of Li, Cs, K, Rb, and Ru slightly decreases the surface area of the catalyst (Uykun Mangaloğlu et al., 2018). The higher loading of the potassium promoter leads to a lower catalytic activity (Jiang et al., 2017a). The promoter may affect the crystal structure of the catalyst, reduction, and carburization process. For example, the researchers employed sodium as a promoter and found that increased loading decreases CO conversion (Buthelezi et al., 2024). During the first stage of the FTS reaction, the sodium promoter alters the electrical characteristics of the Fe-based catalyst, affecting the rate of iron carbide production (Wang et al., 2024). Therefore, the addition of a promoter has a great impact on the catalyst activity (Uykun Mangaloğlu et al., 2018). The efficiency of the promoter depends on the amount of the promoter in the active phase (Horáček, 2020). The selectivity of CO_2 changes in the presence of an iron-based catalyst because it involves the water–gas shift process (Keunecke et al., 2024). To achieve the desired selectivity, the alkali-type promoter and loading need to be optimized (Martinelli et al., 2020a). When the catalyst is evaluated in a slurry bubble column reactor, iron-based catalysts show low resistance to attrition. Low FTS response performance is brought on by inadequate attrition resistance (Buthelezi et al., 2024). Reactor abrasion is an issue for the iron-based catalyst (Keunecke et al., 2024).

3 Cobalt catalyst for FTS

Cobalt (Co) is one of the most studied and utilized transition metals across the board in catalytic applications. Co-based catalysts have seen unprecedented growth in demand in the environment and energy-related sectors for the last few decades, causing the European Union to include them on its list of key raw materials. Co has three empty d-orbitals, whereas nickel and iron have two and four orbitals, respectively. Co forms bonds with incoming chemical species that are neither too strong nor too weak, facilitating the efficient uptake and release of reactants and products (Adeleke et al., 2020). Co has high catalytic activity because its d-orbital is only half-filled. Cobalt occurs in the Co^{2+} and Co^{3+} oxidation states in addition to its elemental form, which facilitates the formation of composites by combining with other elements or supports (Figure 2). The amount of the most stable cobalt oxide (Co_3O_4) can be adjusted by manipulating its redox state, as it consists of two oxidation states, Co^{2+} and Co^{3+}. The ability of cobalt to conduct redox reactions (Co^{2+} to Co^{3+}) makes it an excellent reagent for complex formation since it can provide electrons if the transition state of the process requires them. On the contrary, due to availability of two oxidation states, Co can catch extra electron density if surplus electrons have accumulated during the reaction (Alex et al., 2020). As a result, cobalt species can catalyze reactions involving multiple ions by reacting to generate various ions (Gupta et al., 2023).

Under Fischer–Tropsch reaction conditions, the active phase is not only metallic Co. Still, Co oxides (Qi et al., 2020), carbides of Co, carbon-deposited Co (van Ravenhorst et al., 2018), and Co-support edges (Melaet et al., 2014; Gao et al., 2020) are catalytically active as well. Co oxides are obtained by a calcination process, which is standard practice for synthesizing Co catalysts. However, due to the widespread belief that metallic Co is the premium active phase, Co calcinated samples are reduced or activated in H_2 at high temperatures (Ellis et al., 2019; Wolf et al., 2020).

Co functions at temperatures between 200°C and 250°C, mostly producing linear paraffins (Ten Have and Weckhuysen, 2021). Cobalt's low WGS activity means it works best with feedstocks that have $H_2/CO = 2$, like natural gas. The production of linear alkanes having higher molecular weights and the creation of diesel fuel have been prioritized in the research and development of catalysts for FTS. Co shows strong catalytic activity in the synthesis of paraffin and olefin, in contrast to the predominant products of Fe-based FT catalysts, which are long-chain olefins (Zhai et al., 2021; Ribun et al., 2023).

FIGURE 2
Cobalt properties for suitable FTS catalyst.
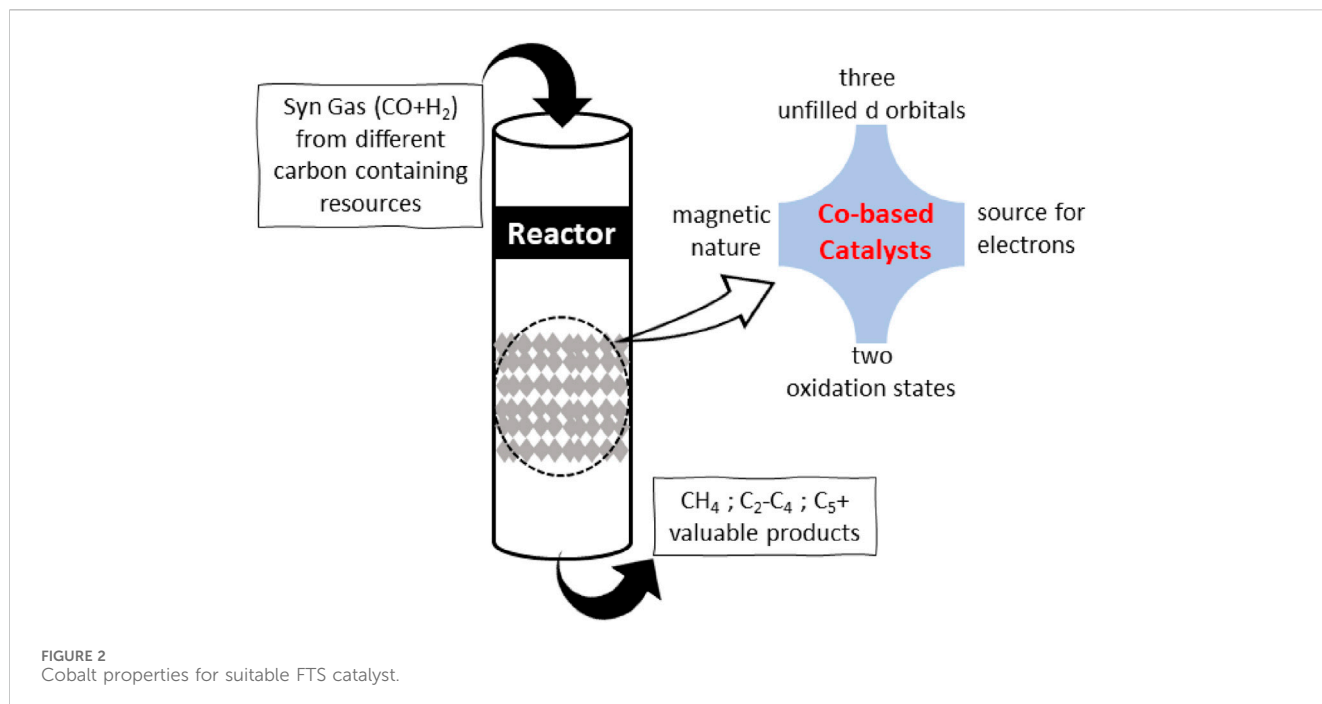
Improved experimental technology and ongoing research have led to the design and production of many high-performing Co-based built-up catalysts. Some have been approved for industrial usage and are in the pilot stage of acceptance. According to reports, Sasol, a global chemical and energy firm, utilized a commercial Co-based catalyst. Using a Co-based catalyst supported on silica with minimal Zr promoter, Royal Shell company (Netherlands) obtained 75% conversion of syngas (CO + H_2) and 82% liquid product selectivity. Alumina- and silica-supported Co catalyst prepared by "Synthroleum" have also shown industrial applications (Suo et al., 2022a).

3.1 Major challenges

The main advantage of oxide-supported Co-based catalysts is the high activity of C-C coupling in the FTS process, making them good candidates for direct conversion of CO to C_{2+} hydrocarbons (Scarfiello et al., 2023). However, the growth of metal crystallites or nanocrystals because of the relocation of metal atoms or clusters driven by thermal energy causes sintering at near 400°C (Moodley et al., 2020). The main disadvantage of oxide-supported Co-based catalysts is the weak CO_2 adsorption and RWGS thermodynamic constraints leading to the CH_4 production and lower hydrocarbons (Van Ravenhorst et al., 2021). Challenges of these catalysts are clarification of the function of CoO and interface between Co^0 and CoO during CO_2-FTS, the possible formation of Co carbide and its effects on CO_2 hydrogenation (Scarfiello et al., 2023). Deactivation is also a key issue with oxide-supported Co-based catalysts. Poisoning, synthesis of support compounds, oxidation, coke deposition, carbide formation, and sintering deactivate Co catalysts supported on oxides. Understanding the sintering mechanism can significantly reduce the sintering rate and improve performance (Rahmati et al., 2020).

Bimetallic Co-based catalysts enhance CO_2 conversion and C_2+ hydrocarbon selectivity over monometallic catalysts. Traditional FTS can boost CO conversion with cobalt, and bimetallic Fe-Co catalysts allow the CO intermediate to spillover from Fe_3O_4 to cobalt sites, allowing CO conversion on both Co and Fe_5C_2 sites (Jiang et al., 2018). However, their synthesis and characterization are more challenging than those of monometallic Co catalysts. Additionally, the addition of a second metal can alter the electronic properties and surface chemistry of the catalyst, which affects its performance and selectivity (Wolf et al., 2021). The primary challenge in bimetallic Co catalysts is to control the distribution and interaction between the two metals, as it has a major impact on the catalyst's performance (van Helden et al., 2020a).

Reducibility of Co catalysts can be increased by addition of a little amount of noble metals (Pt, Ru, Re, and Ag), via forming a larger metallic Co surface on the catalysts, which allows FT reactions to happen at a lower temperature and can significantly upsurge the CO hydrogenation rate, as well as improve CO reactivity and C5+ selectivity (Rahmati et al., 2018; Xu et al., 2020). The addition of these promoters can boost active metal centers. Ru, a structural and electrical promoter, can change the MSI to disperse and reduce Co species. Thus, noble metal-promoted Co catalysts improve reducibility, CO hydrogenation rate, and reaction inherent activity (Suo et al., 2022a). Nevertheless, these metals are expensive, making catalyst production expensive. Additionally, the metal can poison the process if the nanoparticles fuse or become larger, causing mitigation of active sites. There have also been reports concerning the promotion of undesirable reactions for certain metals like hydrogenation or cracking that decrease the production of higher hydrocarbons (Carvalho et al., 2020). Another challenge associated with noble metal-promoted Co catalysts is the promotion of unwanted reactions, such as hydrogenation or cracking. It can reduce selectivity to long-chain hydrocarbons (Suo et al., 2022b).

Non-noble metals, such as iron and nickel, have several advantages when used as promoters for Co-based catalysts. These metals are less expensive than noble metals and can be obtained by more readily available means. In addition, adding these metals can create a strong interaction between the alloy and the support, effectively enhancing catalyst stability. Nickel, for example, can promote CoO reduction and increase stability without the need for high-temperature activation (López-Tinoco et al., 2019). N and p doping also improves catalyst Co particle stability and dispersion (Jacobs et al., 2002; Pedersen et al., 2018). In contrast, adding these cheap promoters can also inhibit the reduction of Co, leading to lower catalytic activity (Liu et al., 2021). The amount of the promoter used for loading should also be considered, as adding more than the optimal amount can negatively affect the CoO reducibility and reduce FTS activity and selectivity (Piao et al., 2020). Furthermore, the strong bond between metal and support by adding of Ni or Fe promotes the cracking reaction, reducing long-chain hydrocarbon selectivity (Martinelli et al., 2020b). The amount of metal promoters must be considered and controlled to maximize the selectivity. Finally, it is crucial to manage the stability of the reduced species to maintain the activity (Shafer et al., 2019).

4 Nickel catalyst for FTS

Nickel (Ni) catalysts play a unique role in the FTS in the production of different ranges of hydrocarbons. However, as per the literature, Fe- and Co-based catalysts are the most used in the FTS process to produce hydrocarbons (Li et al., 2013; Suo et al., 2022b). Though Fe-based catalysts showed good catalytic activity, they suffered from coke formation, leading to catalytic deactivation under operating conditions of 300°C–350°C. However, Co showed good activity toward olefins selectivity, but it also yields more amount of CO_2 due to the dominance of the water–gas shift reaction (Li et al., 2018b). Regarding the Ni catalyst, deactivation occurred at a reaction temperature of 300°C (Li et al., 2018b). Ni is very active for hydrogenation but prone to the formation of coke compared to other active metals (Fe, Co, and Ru), which makes it unsuitable as a direct base catalyst for the FTS application. It also produces volatile carbonyls at the operating reaction conditions to lose a valuable metal during the process (Khodakov et al., 2007). However, Ni as a promoter has been used for Fe- and Co-based catalysts to facilitate the dispersion of the metals, thereby enhancing their activity in the FTS reaction (Feyzi and Akbar Mirzaei, 2010; Rytter et al., 2010; Enger and Holmen, 2012b; López-Tinoco et al., 2020; Chalupka et al., 2021). In addition, Ni can also be replaced over high-cost Ru as a promoter to Co catalysts for better reduction and higher activity (Rytter et al., 2010; Enger and Holmen, 2012b). The catalytic performance in FTS systems was improved over Ni-promoted Co-based catalysts. The influence of Co/Ni ratios on TiO_2, Nb_2O_5, and α-Al_2O_3 supports was studied, and the stable activity and selectivity for long-chain hydrocarbons (C_{5+}) were attained over these Ni-promoted catalysts (Hernández Mejía et al., 2020).

During the FTS reaction, Ni-based catalysts yield more methane than other desired hydrocarbons. From this perspective, Ni as a base catalyst is more active for methane formation from syngas. In countries (China, Japan, Germany, etc.) where natural gas is not readily available, the utilization of syngas derived from coal,

biomass, organic waste, and CO_2 is a viable alternative option as a feedstock for producing synthetic natural gas. Ni, serving as a base catalyst, has demonstrated activity in the synthesis of synthetic natural gas (SNG) from syngas (Enger and Holmen, 2012b; Fan et al., 2014; Gao et al., 2015; Gao et al., 2016; Wang et al., 2016; Wind et al., 2016). Owing to the exothermic characteristics of the CO methanation reaction, the activity is quite lower over that of pure Ni-based catalysts at the lower reaction temperatures. Recently, La-promoted Ni/$MgAl_2O_4$ catalysts exhibited low-temperature activity and high-temperature stability, attributed to smaller Ni particle size, contributing to low-temperature activity, and stronger metal-support interactions, ensuring high-temperature stability (Liu et al., 2020a).

Moreover, the process of converting carbon monoxide (CO) into long-chain hydrocarbons requires significant thermal energy obtained from fossil fuel-derived sources, leading to the release of carbon dioxide (CO_2). In general, CO activation and C–C coupling reactions are required to perform at high reaction temperatures (200°C–400°C) and pressures (2–5 MPa) (Li et al., 2021b). Solar-driven FTS has significant advantages in contrast to conventional FTS, which relies on substantial non-renewable energy inputs (Li et al., 2018b; Wang et al., 2020). The photothermal FTS reaction can utilize solar energy efficiently and tailor the pathways to produce value-added products. Because Ni as an FTS catalyst showed lower activity to yield long-chain hydrocarbons and produces more methane by the methanation reaction, Ni-based photothermal catalysts have been used for FTS reactions to produce C_{2+} hydrocarbons (Wang et al., 2020). The addition of non-metal atoms like O, S, and N, alters the electronic properties of the metal transition nanoparticles and results in good catalytic behavior. However, the phosphidation of TiO_2-supported Ni nanoparticles with transition metal phosphides enhanced the catalytic activity. Titania-supported Ni_2P/Ni catalysts were tested for the photothermal FTS reaction and showed higher selectivity toward C_{2+} hydrocarbons with lower CO conversion (Li et al., 2021b). MnO-supported Ni catalysts were reduced at different temperature ranges (250°C–600°C) and tested for the photothermal FTS reaction. Among all, the Ni-500 (reduced at 500°C) catalyst was reported with 33% olefin selectivity under UV-light irradiation (Wang et al., 2020). Double-layered NiO_x-supported Ni nanoparticles reduced at optimized reduction temperature showed 67.0% selectivity for C_{2+} hydrocarbons and 20.9% conversion achieved due to enhanced C-C coupling reactions over the methanation reaction (Zhao et al., 2016). Ni as a base catalyst, promoter, methanation catalyst, and also as a photothermal catalyst exhibited significant catalytic performance in the CO hydrogenation reaction (FTS route) to produce a different range of hydrocarbons (methane, C_{2+} hydrocarbons, and fuel range hydrocarbons) by tuning their electronic properties and supported with suitable supports (Enger and Holmen, 2012b; Ananikov, 2015; Li et al., 2018b; Li et al., 2021b; Chalupka et al., 2021). Figure 3 shows the role of Ni catalysts in the FTS route to produce different hydrocarbons.

4.1 Major challenges

Ni as a base catalyst in the FTS process yields more saturated hydrocarbons and less emphasis on olefins and other longer-chain hydrocarbons due to their higher hydrogenation affinity. Though Ni

FIGURE 3
Role of the Ni catalyst in the FTS route to produce different hydrocarbons.
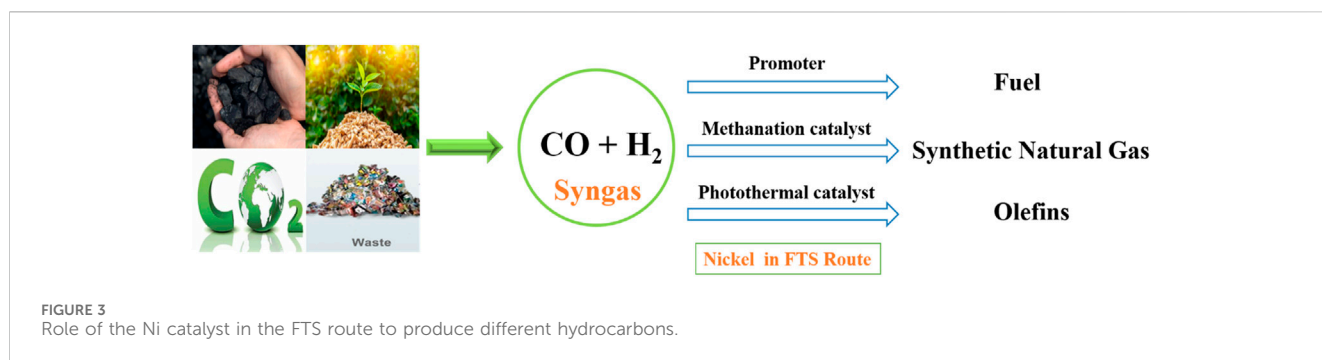
has C-C coupling reactivity, the higher hydrogenation property of Ni must be controlled by tuning the electronic structure of Ni^0 to prevent the hydrogenation of the intermediates (olefins) (Wang et al., 2020).

Ni as a promoter can be replaced over high-cost Ru as a reduction and activity promoter for Fe- and Co-based catalysts. Though the activity was good, it also formed methane due to the high hydrogenation activity. The main challenges associated with the FTS process on Ni-promoted catalysts are CO dissociation, water removal, and chain growth, which all require an optimal balance of a combination of catalytic metal surfaces. (Hernández Mejía et al., 2020). Co-Ni-based alloys showed similar activity as pure Co systems. As the Co cost is higher, it can be used with some cheaper metals (Ni) and yields similar activity. However, finding the right alloy combination and composition is very challenging. In addition, the long-term stability of the Co-Ni alloy must be studied to yield higher selectivity and activity (Van Helden et al., 2020a).

Ni as a methanation catalyst exhibited good activity due to its hydrogenation functionality. However, Ni catalysts showed low activity at lower temperatures for the exothermic nature of the CO methanation reaction due to the accumulation of heat, resulting in the deactivation of the catalyst. Maintaining higher activity at lower temperatures and preventing coke formation are challenges associated with these types of reactions over Ni-based catalysts (Liu et al., 2020b).

In the photothermal FTS system, the presence of Ni_2P on the Ni surface favors thermodynamically occurring C-C coupling reactions, but the formation of methane and CO_2 results in a loss of carbon atom efficiency. Therefore, the selectivity toward C_{5+} and CO conversion needs to be improved (Li et al., 2021b). Ni nanoparticles decorated on NiO_x support exhibited good activity for C_{2+} hydrocarbons rather than the complete formation of methane. Double-layered NiO_x not only absorbs visible light but also prevents methanation and enhances C-C coupling reactions when compared to the Ni metal. Controllable tuning of Ni nanoparticle formation on the doubled-layered NiO_x to enhance CO conversion and the higher yield of olefins and long-chain hydrocarbons are challenging tasks (Zhao et al., 2016).

5 Ruthenium catalyst for FTS

FTS is an exceedingly efficient method for transforming syngas (a mixture of hydrogen and carbon monoxide) into essential chemicals and clean fuels (Li et al., 2018b). As mentioned earlier, the recent escalating crisis of energy has prompted extensive efforts to comprehend the essential elements of FTS, with Ru-, Fe-, and Co-based catalysts widely utilized (Hernández Mejía et al., 2018). Within these catalysts, supported Ru catalysts have exhibited promising potential for FTS due to their inherent high activity and tendency to produce long-chain hydrocarbons (C_{5+}) (Zhang et al., 2020a) selectively. In general, larger particle sizes of Ru-based catalysts, approximately ~8 nm in size, are preferred for FTS (Zhang et al., 2020a). This preference stems from the fact that smaller Ru particles tend to strongly adsorb CO, leading to a preference for methanation rather than the growth of hydrocarbon chains. Ru metal with a suitable particle size promotes CO activation and/or dissociation with or without hydrogen assistance. Hence, Ru-based catalysts have been extensively investigated for FTS to evaluate the impact of surface structure, crystal phase, particle size, and exposed planes of Ru in affecting the catalytic activity and product selectivity (Figure 4).

Various approaches have been utilized recently to improve the performance of Ru-based catalysts. For instance, Ru nanoparticles are placed inside the support to enhance the effectiveness of the catalyst during the FTS. In this regard, Ru incorporation inside the halloysite aluminosilicate nanotubes (HANTs) leads to tubular reactors that are tested for the FTS. Moreover, modification of HANTs using urea, acetone azine, and/or ethylenediaminetetraacetic acid (EDTA) promotes Ru insertion. Further treatment of this modified clay under a reductive environment facilitates a dense population of Ru nanoparticles with 3.5 nm size and 2 wt% loading. These treatments and modifications later play a vital role in the catalytic performance of these catalysts (Stavitskaya et al., 2020). Similarly, incorporating Ru nanoparticles within zeolite pores promotes controlled product selectivity, and zeolite-containing Ru particle catalyst exhibits gasoline selectivity twice that of conventional catalysts (Wang et al., 2021).

Moreover, the regulation of oxide support, e.g., TiO_2 overlayer on Ru under variable reduction conditions, promotes the activity of Ru-based catalysts (Zhang et al., 2020b). The reduction temperature is found to influence CO activation on the oxide support overlayer at the interfaces of the supported Ru catalyst. These findings suggest that the catalyst support and its treatment are crucial in defining their performance during FTS.

The modification of Ru-based catalysts with another transition metal, such as iron and Co, also becomes critical, largely due to the interaction between two parent metals. For instance, in a supported Ru catalyst, the addition of Co doubles the activity (CO conversion); however, despite higher initial conversion, Fe addition to Ru leads to loss of activity with time (Liuzzi et al., 2021). Furthermore, Fe-modified Ru catalyst promotes oxygenate formation as well as CO_2,
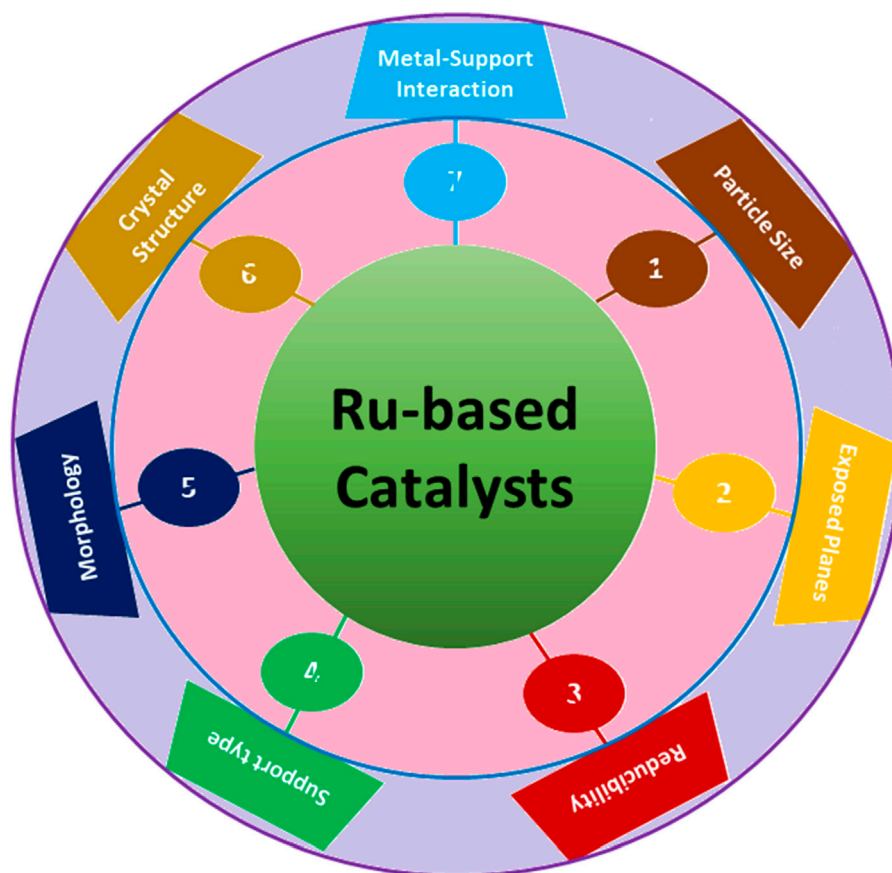
FIGURE 4
Factors affecting the performance of Ru-based catalysts during FTS.

while Co-modified Ru catalysts promote formation of smaller amounts of oxygenate due to smaller metal particle sizes. The surface enrichment with Ru or Co/Fe mainly controls the product selectivity.

The modification of alumina support using citric acid (CA), urea (UR), acetone azine (AA), or ethylenediaminetetraacetic acid (EDTA) for Ru- and Co-based bimetallic catalysts showed that the catalyst characteristics such as surface atom composition, metal dispersion, extent of acidic sites, and reducibility are a function of modifying agents. The CA-modified alumina-supported catalyst (Ru-Co-Al) exhibited lower activity and formation of mainly solid paraffins. EDTA modification promoted gasoline selectivity, while the AA-modified catalyst showed higher selectivity to diesel. The UR-modified catalyst remained the optimal performing catalyst with 37.3% CO conversion and C_{5+} selectivity of 79.4%. UR modification facilitated the formation of Ru-Co alloy, leading to better reducibility and moderate acidity that played a role in optimal performance of this catalyst (Mazurova et al., 2024).

5.1 Major challenges

The Ru size variation promotes suitable metal–support interaction that positively influences the chain growth during

FTS (Zhang et al., 2020a). However, despite an increase in activity with an increase in Ru particle size, C_{5+} selectivity is reduced (Zhang et al., 2020a). Controlling the Ru particle size close to 8 nm is crucial to attain higher activity and selectivity (Zhang et al., 2020a) as larger Ru particles tend to promote undesired methanation reactions (Zhang et al., 2020a). The catalyst's rational design at the micro level, facilitating both higher activity and desired long-chain product selectivity, remains challenging (Sun et al., 2023).

The variation in metal–support interaction (MSI) as a function of Ru size can tune the reduction behavior as well as the reactivity during FTS (Zhang et al., 2020a). Both the support type and Ru metal contents play a role in reducing the activity and product selectivity (Yan et al., 2020). Stronger MSI in the case of Ru supported on reducible oxide support such as TiO_2 promotes surface active site enrichment (Zhang et al., 2020b). It is difficult to fine-tune the metal–zeolite bifunctional catalyst design in a nanocomposite zeolite catalyst to produce gasoline-type fuels because of the metal–acid site closeness (Přech et al., 2020).

In case of supported catalysts, the oxide support overlayer envelops Ru nanoparticles and promotes CO dissociation (Zhang et al., 2020b). In modified aluminosilicate support catalysts, the specific morphology and total acidity are major factors affecting the catalytic activity and product selectivity (Stavitskaya et al., 2020). The urea-modified aluminosilicate-supported Ru catalyst

demonstrates high selectivity toward C_{5+} (Stavitskaya et al., 2020). Though the carbon aerogel-supported Ru catalyst shows higher activity, the catalyst shows no stability (Zhang et al., 2022). Furthermore, the ethylenediaminetetraacetic acid-modified aluminosilicate supported catalyst promoted the methanation reaction (Stavitskaya et al., 2020). In the case of zeolite-supported Ru catalysts, Ru nanoparticles placed inside zeolite crystals tune product selectivity (Wang et al., 2021). In spite of this, the metal encapsulated in zeolite comes out and agglomerates, leading to loss of activity (Liuzzi et al., 2021). Appropriate metal–support interaction that maintains the structure of single crystals is critical (Cheng et al., 2021).

In a promoted Ru catalyst, the role of metal–support interaction becomes prominent in comparison with the metal–promoter interaction and retaining the proximity between the promoter and Ru facilitates Lewis acidity, which, in turn, promotes CO dissociation (Eslava et al., 2020). Higher dispersion with the addition of a second metal, such as cobalt, to a Ru-based catalyst promotes activity (Liuzzi et al., 2021). Therefore, the choice of a second metal is critical in influencing the selectivity and yield of undesired products (Liuzzi et al., 2021).

The manganese promotional impact on the catalytic performance of Ru-based catalyst supported on silica revealed that manganese addition not only suppressed the formation of methane and second-stage olefin hydrogenation but also promoted activity as well as formation of long-chain olefins. Moreover, manganese addition played a role in enhancing the dispersion of Ru nanoparticles as well as the electron density of Ru active sites, leading to increased adsorption of CO followed by enhanced CO dissociation (An et al., 2023).

6 Future recommendations

Future studies should focus on improving the performance of iron-based catalysts such that the reduction behavior and the surface basicity of the catalysts need to be improved for higher catalyst activity and hydrocarbon selectivity. Low-cost and eco-friendly methods for the preparation of high-temperature (HT-FTS)-based iron catalysts are available, but the low-temperature (LT-FTS)-based iron catalyst needs to be addressed. The LT-FTS-based iron catalysts exhibit poor textural properties for the iron particles. It is suggested that all Co uses be strictly monitored to prevent any accidental discharge into the environment, particularly water supplies. Co toxicity, especially from used catalysts, influences living things and should be studied so that appropriate precautions can be taken. The emphasis on Ni as a catalyst for FTS reaction is still craving to address the drawbacks of this process by optimizing particle size in the nanorange and exploring different bimetallic combinations to enhance the selectivity and activity. In addition, it can be explored by integrating computational tools to design better catalyst composition efficiently. In the case of Ru-based catalysts, particle size and oxide support play a vital role in tuning the performance of the catalysts during FTS, specifically for product selectivity. The various reports on the impact of particle sizes demand further investigation on this aspect of Ru-based catalysts.

Due to the contribution of factors such as support type, electronic effects, or deactivation impacts, the potential performance of Ru-based catalysts still needs to be fully evaluated, which requires to be explored in the future. The metal–support interaction manifests in various ways depending upon oxide support type, chemical composition, size of metal particles, and charge transfer. The complexity of these factors combined requires rigorous evaluation of this aspect in the FTS. In order to gain insights into the metal–support interaction at the micro level, theoretical techniques such as density functional theory (DFT) are handy. However, the disparity between experimental and theoretical data is a challenge.

7 Conclusion

The iron-based catalysts are cheap as compared to other FTS processes. The formation of Fe_2C and Fe_5C_2 creates difficulty for the formation of the Fe_7C_3 phase, which is considered to be a more active phase for iron-based FTS catalysts. In the near future, we will require novel *in situ* practices to enhance our understanding of actual catalyst structures under FTS conditions. Theoretical investigations, particularly those based on artificial intelligence (AI) approaches, are proposed to understand further the nature of the available active sites and reaction mechanisms in Co-based FTS processes.

The advantage and disadvantage of Ni as an FTS catalyst include having high hydrogenation activity, which yields more methane and limits longer hydrocarbons. However, Ni can be used as a promoter and methanation catalyst and also can be used as a photothermal FTS catalyst to yield different hydrocarbons by tuning the physicochemical properties. Ru-based catalysts with a suitable particle size perform exceptionally during the FTS. The smaller particles tend to show lower activity due to site blockage on the corners/edges, along with metal agglomeration.

In comparison, larger particles close to 8 nm are ideal for the excellent performance of the catalysts. Metal–support interaction is also found to have a vital role in influencing the catalytic performance. In summary, all iron, cobalt, nickel, and ruthenium-based catalysts demonstrate key issues and challenges that are required to be addressed to achieve catalysts with better catalytic performance as well as targeting desired product selectivity.

Author contributions

MA: conceptualization, investigation, writing–original draft, and writing–review and editing. MU: conceptualization, data curation, investigation, and writing–original draft. TK: conceptualization, data curation, formal analysis, and writing–original draft. WK: conceptualization, data curation, formal analysis, validation, and writing–original draft. IK: conceptualization, data curation, formal analysis, and writing–original draft. KH: funding acquisition, resources, supervision, validation, writing–original draft, and writing–review and editing.

Funding

Acknowledgments

Conflict of interest

The authors declare that the research was conducted in the absence of any commercial or financial relationships that could be construed as a potential conflict of interest.

Publisher's note

All claims expressed in this article are solely those of the authors and do not necessarily represent those of their affiliated organizations, or those of the publisher, the editors, and the reviewers. Any product that may be evaluated in this article, or claim that may be made by its manufacturer, is not guaranteed or endorsed by the publisher.

References

Abbasi, M., Mirzaei, A. A., and Atashi, H. (2019). Hydrothermal synthesis of Fe-Ni-Ce nano-structure catalyst for Fischer-Tropsch synthesis: characterization and catalytic performance. *J. Alloys Compd.* 799, 546–555. doi:10.1016/J.JALLCOM.2019.05.314

Adeleke, A. A., Liu, X., Lu, X., Moyo, M., and Hildebrandt, D. (2020). Cobalt hybrid catalysts in Fischer-Tropsch synthesis. *Rev. Chem. Eng.* 36, 437–457. doi:10.1515/revce-2018-0012

Adnan, M. A., Hidayat, A., Hossain, M. M., and Muraza, O. (2021). Transformation of low-rank coal to clean syngas and power via thermochemical route. *Energy* 236, 121505. doi:10.1016/j.energy.2021.121505

Alex, C., Sarma, S. C., Peter, S. C., and John, N. S. (2020). Competing effect of Co3+Reducibility and oxygen-deficient defects toward high oxygen evolution activity in Co3O4Systems in alkaline medium. *ACS Appl. Energy Mater* 3, 5439–5447. doi:10.1021/acsaem.0c00297

Amin, M., Munir, S., Iqbal, N., Wabaidur, S. M., and Iqbal, A. (2022a). The conversion of waste biomass into carbon-supported iron catalyst for syngas to clean liquid. *Fuel Prod.*, 1–14. doi:10.3390/catal12101234

Amin, M., Shah, H. H., Fareed, A. G., Khan, W. U., Chung, E., Zia, A., et al. (2022b). Hydrogen production through renewable and non-renewable energy processes and their impact on climate change. *Int. J. Hydrogen Energy* 47, 33112–33134. doi:10.1016/j.ijhydene.2022.07.172

Amin, M., Shah, H. H., Naveed, A. B., Iqbal, A., Gamil, Y., and Najeh, T. (2024). Life cycle assessment of iron-biomass supported catalyst for Fischer Tropsch synthesis. *Front. Chem.* 12, 1374739. doi:10.3389/fchem.2024.1374739

An, Y., Wang, X., Yu, H., Qi, X., Lv, D., Lin, T., et al. (2023). Mn-promoted Ru-based catalysts for enhanced fischer-tropsch synthesis of olefins from syngas. *ACS Catal.* 13, 13245–13256. doi:10.1021/ACSCATAL.3C03455/SUPPL_FILE/CS3C03455_SI_001

Ananikov, V. P. (2015). Nickel: the "spirited horse" of transition metal catalysis. *ACS Catal.* 5, 1964–1971. doi:10.1021/acscatal.5b00072

Badoga, S., Kamath, G., and Dalai, A. (2020). Effects of promoters (Mn, Mg, Co and Ni) on the Fischer-Tropsch activity and selectivity of KCuFe/mesoporous-alumina catalyst. *Appl. Catal. A Gen.* 607, 117861. doi:10.1016/j.apcata.2020.117861

Bice, D. (2023). Global energy sources.

Buthelezi, A. S., Tucker, C. L., Heeres, H. J., Shozi, M. L., van de Bovenkamp, H. H., and Ntola, P. (2024). Fischer-tropsch synthesis using promoted, unsupported, supported, bimetallic and spray-dried iron catalysts: a review. *Results Chem.* 9, 101623. doi:10.1016/J.RECHEM.2024.101623

Carvalho, A., Ordomsky, V. V., Marcilio, N. R., and Khodakov, A. Y. (2020). Number and intrinsic activity of cobalt surface sites in platinum promoted zeolite catalysts for carbon monoxide hydrogenation. *Catal. Sci. Technol.* 10, 2137–2144. doi:10.1039/C9CY02421B

Chalupka, K. A., Sadek, R., Szkudlarek, L., Mierczynski, P., Maniukiewicz, W., Rynkowski, J., et al. (2021). The catalytic activity of microporous and mesoporous NiCoBeta zeolite catalysts in Fischer–Tropsch synthesis. *Res. Chem. Intermed.* 47, 397–418. doi:10.1007/s11164-020-04343-0

Chen, Y., Ma, L., Zhang, R., Ye, R., Liu, W., Wei, J., et al. (2022). Carbon-supported Fe catalysts with well-defined active sites for highly selective alcohol production from Fischer-Tropsch synthesis. *Appl. Catal. B* 312, 121393. doi:10.1016/j.apcatb.2022.121393

Chen, Y., Wei, J., Duyar, M. S., Ordomsky, V. V., Khodakov, A. Y., and Liu, J. (2021). Carbon-based catalysts for Fischer-Tropsch synthesis. *Chem. Soc. Rev.* 50, 2337–2366. doi:10.1039/d0cs00905a

Cheng, Q., Liu, Y., Lyu, S., Tian, Y., Ma, Q., and Li, X. (2021). Manipulating metal-support interactions of metal catalysts for Fischer-Tropsch synthesis. *Chin. J. Chem. Eng.* 35, 220–230. doi:10.1016/j.cjche.2021.05.013

Chernyak, S. A., Ivanov, A. S., Maksimov, S. V., Maslakov, K. I., Isaikina, O. Y., Chernavskii, P. A., et al. (2020). Fischer-Tropsch synthesis over carbon-encapsulated cobalt and iron nanoparticles embedded in 3D-framework of carbon nanotubes. *J. Catal.* 389, 270–284. doi:10.1016/j.jcat.2020.06.011

Chun, D. H., Rhim, G. B., Youn, M. H., Deviana, D., Lee, J. E., Park, J. C., et al. (2020). Brief review of precipitated iron-based catalysts for low-temperature fischer–tropsch synthesis. *Top. Catal.* 63, 793–809. doi:10.1007/s11244-020-01336-6

Davis, B. H. (2009). Fischer-Tropsch Synthesis: reaction mechanisms for iron catalysts. *Catal. Today* 141, 25–33. doi:10.1016/j.cattod.2008.03.005

De, S., Zhang, J., Luque, R., and Yan, N. (2016). Ni-based bimetallic heterogeneous catalysts for energy and environmental applications. *Energy Environ. Sci.* 9, 3314–3347. doi:10.1039/C6EE02002J

Di, Z., Feng, X., Yang, Z., and Luo, M. (2020). Effect of iron precursor on catalytic performance of precipitated iron catalyst for fischer–tropsch synthesis reaction. *Catal. Lett.* 150, 2640–2647. doi:10.1007/s10562-020-03158-3

Edla, R., Gupta, S., Patel, N., Bazzanella, N., Fernandes, R., Kothari, D. C., et al. (2016). Enhanced H2 production from hydrolysis of sodium borohydride using Co3O4 nanoparticles assembled coatings prepared by pulsed laser deposition. *Appl. Catal. A Gen.* 515, 1–9. doi:10.1016/J.APCATA.2016.01.031

Einemann, M., Neumann, F., and Roessner, F. (2024). Influence of ammonia and different promoters on the iron-based fischer-tropsch synthesis. *ChemCatChem*, e202400726. doi:10.1002/CCTC.202400726

Ellis, P. R., Enache, D. I., James, D. W., Jones, D. S., and Kelly, G. J. (2019). A robust and precious metal-free high performance cobalt Fischer–Tropsch catalyst. *Nat. Catal.* 2, 623–631. doi:10.1038/s41929-019-0288-5

Enger, B. C., and Holmen, A. (2012a). Nickel and fischer-tropsch synthesis. *Catal. Rev.* 54, 437–488. doi:10.1080/01614940.2012.670088

Enger, B. C., and Holmen, A. (2012b). Nickel and fischer-tropsch synthesis. *Catal. Rev. Sci. Eng.* 54, 437–488. doi:10.1080/01614940.2012.670088

Eslava, J. L., Gallegos-Suárez, E., Guerrero-Ruiz, A., and Rodríguez-Ramos, I. (2020). Effect of Mo promotion on the activity and selectivity of Ru/Graphite catalysts for Fischer-Tropsch synthesis. *Catal. Today* 357, 185–192. doi:10.1016/j.cattod.2019.05.051

Fan, M. T., Miao, K. P., Lin, J. D., Zhang, H. B., and Liao, D. W. (2014). Mg-Al oxide supported Ni catalysts with enhanced stability for efficient synthetic natural gas from syngas. *Appl. Surf. Sci.* 307, 682–688. doi:10.1016/j.apsusc.2014.04.098

Feyzi, M., and Akbar Mirzaei, A. (2010). Performance and characterization of iron-nickel catalysts for light olefin production. *J. Nat. Gas Chem.* 19, 422–430. doi:10.1016/S1003-9953(09)60092-X

Fu, X. P., Yu, W. Z., Ma, C., Lin, J., Sun, S. Q., Li, S. Q., et al. (2021). Supported Fe2C catalysts originated from Fe2N phase and active for Fischer-Tropsch synthesis. *Appl. Catal. B* 284, 119702. doi:10.1016/j.apcatb.2020.119702

Gao, J., Liu, Q., Gu, F., Liu, B., Zhong, Z., and Su, F. (2015). Recent advances in methanation catalysts for the production of synthetic natural gas. *RSC Adv.* 5, 22759–22776. doi:10.1039/c4ra16114a

Gao, L., Fu, Q., Wei, M., Zhu, Y., Liu, Q., Crumlin, E., et al. (2016). Enhanced nickel-catalyzed methanation confined under hexagonal boron nitride shells. *ACS Catal.* 6, 6814–6822. doi:10.1021/acscatal.6b02188

Gao, P., Zhang, L., Li, S., Zhou, Z., and Sun, Y. (2020). Novel heterogeneous catalysts for CO2 hydrogenation to liquid fuels. *ACS Cent. Sci.* 6, 1657–1670. doi:10.1021/ACSCENTSCI.0C00976

Gupta, S., Fernandes, R., Patel, R., Spreitzer, M., and Patel, N. (2023). A review of cobalt-based catalysts for sustainable energy and environmental applications. *Appl. Catal. A Gen.* 661, 119254. doi:10.1016/j.apcata.2023.119254

Hernández Mejía, C., van Deelen, T. W., and de Jong, K. P. (2018). Activity enhancement of cobalt catalysts by tuning metal-support interactions. *Nat. Commun.* 9, 4459. doi:10.1038/s41467-018-06903-w

Hernández Mejía, C., Van Der Hoeven, J. E. S., De Jongh, P. E., and De Jong, K. P. (2020). Cobalt-nickel nanoparticles supported on reducible oxides as fischer-tropsch catalysts. *ACS Catal.* 10, 7343–7354. doi:10.1021/acscatal.0c00777

Horáček, J. (2020). Fischer–Tropsch synthesis, the effect of promoters, catalyst support, and reaction conditions selection. *Monatsh Chem.* 151, 649–675. doi:10.1007/s00706-020-02590-w

Jacobs, G., Das, T. K., Zhang, Y., Li, J., Racoillet, G., and Davis, B. H. (2002). Fischer-Tropsch synthesis: support, loading, and promoter effects on the reducibility of cobalt catalysts. *Appl. Catal. A Gen.* 233, 263–281. doi:10.1016/S0926-860X(02)00195-3

Jiang, F., Liu, B., Geng, S., Xu, Y., and Liu, X. (2018). Hydrogenation of CO2 into hydrocarbons: enhanced catalytic activity over Fe-based Fischer–Tropsch catalysts. *Catal. Sci. Technol.* 8, 4097–4107. doi:10.1039/C8CY00850G

Jiang, F., Zhang, M., Liu, B., Xu, Y., and Liu, X. (2017a). Insights into the influence of support and potassium or sulfur promoter on iron-based Fischer-Tropsch synthesis: understanding the control of catalytic activity, selectivity to lower olefins, and catalyst deactivation. *Catal. Sci. Technol.* 7, 1245–1265. doi:10.1039/c7cy00048k

Keunecke, A., Dossow, M., Dieterich, V., Spliethoff, H., and Fendt, S. (2024). Insights into Fischer–Tropsch catalysis: current perspectives, mechanisms, and emerging trends in energy research. *Front. Energy Res.* 12. doi:10.3389/fenrg.2024.1344179

Khodakov, A. Y., Chu, W., and Fongarland, P. (2007). Advances in the development of novel cobalt Fischer–Tropsch catalysts for synthesis of long-chain hydrocarbons and clean fuels. *Chem. Rev.* 107, 1692–1744. doi:10.1021/cr050972v

Krzyszczak, A., Dybowski, M. P., and Czech, B. (2021). Formation of polycyclic aromatic hydrocarbons and their derivatives in biochars: the effect of feedstock and pyrolysis conditions. *J. Anal. Appl. Pyrolysis* 160, 105339. doi:10.1016/j.jaap.2021.105339

Li, J., He, Y., Tan, L., Zhang, P., Peng, X., Oruganti, A., et al. (2018a). Integrated tuneable synthesis of liquid fuels via Fischer–Tropsch technology. *Nat. Catal.* 1, 787–793. doi:10.1038/s41929-018-0144-z

Li, J., Zhang, C., Cheng, X., Qing, M., Xu, J., Wu, B., et al. (2013). Effects of alkaline-earth metals on the structure, adsorption and catalytic behavior of iron-based Fischer–Tropsch synthesis catalysts. *Appl. Catal. A Gen.* 464–465, 10–19. doi:10.1016/J.APCATA.2013.04.042

Li, X., Chen, Y., Liu, S., Zhao, N., Jiang, X., Su, M., et al. (2021a). Enhanced gasoline selectivity through Fischer-Tropsch synthesis on a bifunctional catalyst: effects of active sites proximity and reaction temperature. *Chem. Eng. J.* 416, 129180. doi:10.1016/j.cej.2021.129180

Li, Z., Liu, J., Zhao, Y., Waterhouse, G. I. N., Chen, G., Shi, R., et al. (2018b). Co-based catalysts derived from layered-double-hydroxide nanosheets for the photothermal production of light olefins. *Adv. Mater.* 30, e1800527–e1800528. doi:10.1002/adma.201800527

Li, Z., Zhang, X., Liu, J., Shi, R., Waterhouse, G. I. N., Wen, X. D., et al. (2021b). Titania-supported Ni2P/Ni catalysts for selective solar-driven CO hydrogenation. *Adv. Mater.* 33, e2103248–8. doi:10.1002/adma.202103248

Liu, Q., Sun, J., Feng, Q., Ji, S., and Wang, Z. jun (2020a). A La-promoted Ni/MgAl2O4 catalyst with superior methanation performance for the production of synthetic natural gas. *Catal. Today* 339, 127–134. doi:10.1016/j.cattod.2019.07.034

Liu, Q., Sun, J., Feng, Q., Ji, S., and Wang, Z. jun (2020b). A La-promoted Ni/MgAl2O4 catalyst with superior methanation performance for the production of synthetic natural gas. *Catal. Today* 339, 127–134. doi:10.1016/J.CATTOD.2019.07.034

Liu, Q. Y., Shang, C., and Liu, Z. P. (2022). *In situ* active site for Fe-catalyzed fischer-tropsch synthesis: recent progress and future challenges. *J. Phys. Chem. Lett.* 13, 3342–3352. doi:10.1021/acs.jpclett.2c00549

Liu, Y., Chen, Y., Yu, H., Guan, F., Hou, Z., Cui, D., et al. (2021). Bimetallic Ni-Co catalysts for co-production of methane and liquid fuels from syngas. *Catal. Today* 369, 167–174. doi:10.1016/J.CATTOD.2020.05.011

Liuzzi, D., Pérez-Alonso, F. J., and Rojas, S. (2021). Ru-M (M = Fe or Co) Catalysts with high Ru surface concentration for Fischer-Tropsch synthesis. *Fuel* 293, 120435. doi:10.1016/j.fuel.2021.120435

López-Tinoco, J., Mendoza-Cruz, R., Bazán-Díaz, L., Karuturi, S. C., Martinelli, M., Cronauer, D. C., et al. (2019). The preparation and characterization of Co–Ni nanoparticles and the testing of a heterogenized Co–Ni/alumina catalyst for CO hydrogenation. *Catal. 2020* 10, 18. doi:10.3390/CATAL10010018

López-Tinoco, J., Mendoza-Cruz, R., Bazán-Díaz, L., Karuturi, S. C., Martinelli, M., Cronauer, D. C., et al. (2020). The preparation and characterization of co–ni

nanoparticles and the testing of a heterogenized co–ni/alumina catalyst for co hydrogenation. *Catalysts* 10, 18. doi:10.3390/catal10010018

Lu, F., Chen, X., Lei, Z., Wen, L., and Zhang, Y. (2021a). Revealing the activity of different iron carbides for Fischer-Tropsch synthesis. *Appl. Catal. B* 281, 119521. doi:10.1016/j.apcatb.2020.119521

Lu, F., Chen, X., Wen, L., Wu, Q., and Zhang, Y. (2021b). The synergic effects of iron carbides on conversion of syngas to alkenes. *Catal. Lett.* 151, 2132–2143. doi:10.1007/s10562-020-03505-4

Ma, C., Zhang, W., Chang, Q., Wang, X., Wang, H., Chen, H., et al. (2021b). θ-Fe3C dominated Fe@C core–shell catalysts for Fischer-Tropsch synthesis: roles of θ-Fe3C and carbon shell. *J. Catal.* 393, 238–246. doi:10.1016/j.jcat.2020.11.033

Martinelli, M., Gnanamani, M. K., LeViness, S., Jacobs, G., and Shafer, W. D. (2020a). An overview of Fischer-Tropsch Synthesis: XtL processes, catalysts and reactors. *Appl. Catal. A Gen.* 608, 117740. doi:10.1016/j.apcata.2020.117740

Martinelli, M., Karuturi, S. C., Garcia, R., Watson, C. D., Shafer, W. D., Cronauer, D. C., et al. (2020b). Substitution of Co with Ni in Co/Al2O3 catalysts for fischer–tropsch synthesis. *Catal. 2020* 10, 334–410. doi:10.3390/CATAL10030334

Mazurova, K., Miyassarova, A., Eliseev, O., Yakovenko, R., Kazantsev, R., Glotov, A., et al. (2024). Fischer–Tropsch synthesis over RuCo catalysts: an effect of ligands on the active phase properties and catalytic activity. *Chem. Eng. J.* 488, 150837. doi:10.1016/J.CEJ.2024.150837

Melaet, G., Ralston, W. T., Li, C. S., Alayoglu, S., An, K., Musselwhite, N., et al. (2014). Evidence of highly active cobalt oxide catalyst for the Fischer-Tropsch synthesis and CO2 hydrogenation. *J. Am. Chem. Soc.* 136, 2260–2263. doi:10.1021/ja412447q

Moodley, D., Claeys, M., van Steen, E., van Helden, P., Kistamurthy, D., Weststrate, K. J., et al. (2020). Sintering of cobalt during FTS: insights from industrial and model systems. *Catal. Today* 342, 59–70. doi:10.1016/J.CATTOD.2019.03.059

Nanduri, A., and Mills, P. L. (2020). Effect of catalyst shape and multicomponent diffusion flux models on intraparticle transport-kinetic interactions in the gas-phase Fischer-Tropsch synthesis. *Fuel* 278, 118117. doi:10.1016/j.fuel.2020.118117

Nayak, S. K., Hoang, A. T., Nižetić, S., Nguyen, X. P., and Le, T. H. (2022). Effects of advanced injection timing and inducted gaseous fuel on performance, combustion and emission characteristics of a diesel engine operated in dual-fuel mode. *Fuel* 310, 122232–122316. doi:10.1016/j.fuel.2021.122232

Nie, C., Zhang, H., Ma, H., Qian, W., Sun, Q., and Ying, W. (2019). Effects of Ce addition on Fe–Cu catalyst for fischer–tropsch synthesis. *Catal. Lett.* 149, 1375–1382. doi:10.1007/s10562-019-02700-2

Pedersen, E. Ø., Svenum, I. H., and Blekkan, E. A. (2018). Mn promoted Co catalysts for Fischer-Tropsch production of light olefins – an experimental and theoretical study. *J. Catal.* 361, 23–32. doi:10.1016/j.jcat.2018.02.011

Piao, Y., Jiang, Q., Li, H., Matsumoto, H., Liang, J., Liu, W., et al. (2020). Identify Zr promotion effects in atomic scale for Co-based catalysts in fischer-tropsch synthesis. *ACS Catal.* 10, 7894–7906. doi:10.1021/acscatal.0c01874

Popat, Y., Orlandi, M., Patel, N., Edla, R., Bazzanella, N., Gupta, S., et al. (2019). Pulsed laser deposition of CoFe2O4/CoO hierarchical-type nanostructured heterojuction forming a Z-scheme for efficient spatial separation of photoinduced electron-hole pairs and highly active surface area. *Appl. Surf. Sci.* 489, 584–594. doi:10.1016/J.APSUSC.2019.05.314

Přech, J., Strossi Pedrolo, D. R., Marcilio, N. R., Gu, B., Peregudova, A. S., Mazur, M., et al. (2020). Core–Shell metal zeolite composite catalysts for *in situ* processing of fischer–tropsch hydrocarbons to gasoline type fuels. *ACS Catal.* 10, 2544–2555. doi:10.1021/acscatal.9b04421

Qi, Z., Chen, L., Zhang, S., Su, J., and Somorjai, G. A. (2020). A mini review of cobalt-based nanocatalyst in Fischer-Tropsch synthesis. *Appl. Catal. A Gen.* 602, 117701. doi:10.1016/J.APCATA.2020.117701

Rahmati, M., Huang, B., Schofield, L. M., Fletcher, T. H., Woodfield, B. F., Hecker, W. C., et al. (2018). Effects of Ag promotion and preparation method on cobalt Fischer-Tropsch catalysts supported on silica-modified alumina. *J. Catal.* 362, 118–128. doi:10.1016/J.JCAT.2018.03.027

Rahmati, M., Safdari, M. S., Fletcher, T. H., Argyle, M. D., and Bartholomew, C. H. (2020). Chemical and thermal sintering of supported metals with emphasis on cobalt catalysts during fischer-tropsch synthesis. *Chem. Rev.* 120, 4455–4533. doi:10.1021/acs.chemrev.9b00417

Ribun, V., Boichenko, S., and Kale, U. (2023). Advances in gas-to-liquid technology for environmentally friendly fuel synthesis: analytical review of world achievements. *Energy Rep.* 9, 5500–5508. doi:10.1016/j.egyr.2023.04.372

Rytter, E., Skagseth, T. H., Eri, S., and Sjåstad, A. O. (2010). Cobalt fischer-tropsch catalysts using nickel promoter as a rhenium substitute to suppress deactivation. *Ind. Eng. Chem. Res.* 49, 4140–4148. doi:10.1021/ie100308f

Scarfiello, C., Pham Minh, D., Soulantica, K., and Serp, P. (2023). Oxide supported cobalt catalysts for CO2 hydrogenation to hydrocarbons: recent progress. *Adv. Mater Interfaces* 10. doi:10.1002/admi.202202516

Shafer, W. D., Gnanamani, M. K., Graham, U. M., Yang, J., Masuku, C. M., Jacobs, G., et al. (2019). Fischer-tropsch: product selectivity-the fingerprint of synthetic fuels. *Catalysts* 9, 259. doi:10.3390/CATAL9030259

Shah, H. H., Amin, M., and Pepe, F. (2023). Maximizing resource efficiency: opportunities for energy recovery from municipal solid waste in Europe. *J. Mater Cycles Waste Manag.* 25, 2766–2782. doi:10.1007/s10163-023-01733-5

Song, X., Zhang, X., hui, Q., Xu, J. yu, ye, X., and Chen, A. cheng (2021). Intrinsic support effects on the catalytic performances during Fischer–Tropsch synthesis over well-defined uniform pore-structure Fe-based catalysts. *React. Kinet. Mech. Catal.* 133, 983–996. doi:10.1007/s11144-021-02036-2

Stavitskaya, A., Mazurova, K., Kotelev, M., Eliseev, O., Gushchin, P., Glotov, A., et al. (2020). Ruthenium-loaded halloysite nanotubes as mesocatalysts for fischer–tropsch synthesis. *Molecules* 25, 1764. doi:10.3390/molecules25081764

Sun, J., Tao, L., Ye, C., Wang, Y., Meng, G., Lei, H., et al. (2023). MOF-derived Ru1Zr1/Co dual-atomic-site catalyst with promoted performance for fischer–tropsch synthesis. *J. Am. Chem. Soc.* 145, 7113–7122. doi:10.1021/jacs.2c09168

Suo, Y., Yao, Y., Zhang, Y., Xing, S., and Yuan, Z. Y. (2022a). Recent advances in cobalt-based Fischer-Tropsch synthesis catalysts. *J. Industrial Eng. Chem.* 115, 92–119. doi:10.1016/j.jiec.2022.08.026

Suo, Y., Yao, Y., Zhang, Y., Xing, S., and Yuan, Z. Y. (2022b). Recent advances in cobalt-based Fischer-Tropsch synthesis catalysts. *J. Industrial Eng. Chem.* 115, 92–119. doi:10.1016/J.JIEC.2022.08.026

Ten Have, I. C., and Weckhuysen, B. M. (2021). The active phase in cobalt-based Fischer-Tropsch synthesis. *Chem. Catal.* 1, 339–363. doi:10.1016/j.checat.2021.05.011

Torres Galvis, H. M., and De Jong, K. P. (2013). Catalysts for production of lower olefins from synthesis gas: a review. *ACS Catal.* 3, 2130–2149. doi:10.1021/cs4003436

Usman, M., Fareed, A. G., and Amin, M. (2024). A bibliometric analysis of CO2 methanation: research trends and comprehension of effective catalysts. *J. Iran. Chem. Soc.* 21, 1185–1201. doi:10.1007/s13738-024-02998-9

Uykun Mangaloğlu, D., Baranak, M., Ataç, Ö., and Atakül, H. (2018). Effect of the promoter presence in catalysts on the compositions of Fischer–Tropsch synthesis products. *J. Industrial Eng. Chem.* 66, 298–310. doi:10.1016/j.jiec.2018.05.044

Van de Loosdrecht, J., Botes, F. G., Ciobica, I. M., Ferreira, A., Gibson, P., Moodley, D. J., et al. (2013). Fischer–Tropsch synthesis: catalysts and chemistry. *Compr. Inorg. Chem. II Elem. Appl.* 7, 525–557. doi:10.1016/B978-0-08-097774-4.00729-4

van Helden, P., Prinsloo, F., van den Berg, J. A., Xaba, B., Erasmus, W., Claeys, M., et al. (2020a). Cobalt-nickel bimetallic Fischer-Tropsch catalysts: a combined theoretical and experimental approach. *Catal. Today* 342, 88–98. doi:10.1016/J.CATTOD.2019.03.001

Van Ravenhorst, I. K., Hoffman, A. S., Vogt, C., Boubnov, A., Patra, N., Oord, R., et al. (2021). On the cobalt carbide formation in a Co/TiO2 fischer-tropsch synthesis catalyst as studied by high-pressure, long-term operando X-ray absorption and diffraction. *ACS Catal.* 11, 2956–2967. doi:10.1021/acscatal.0c04695

van Ravenhorst, I. K., Vogt, C., eiko Oosterbeek, H., Bossers, K. W., osØ Moya-Cancino, J. G., lexander van Bavel, A. P., et al. (2018). Capturing the genesis of an active fischer–tropsch synthesis catalyst with operando X-ray nanospectroscopy. *Angew. Chem. Int. Ed.* 57, 11957–11962. doi:10.1002/ANIE.201806354

Wang, C., Fang, W., Wang, L., and Xiao, F.-S. (2021). Fischer-Tropsch reaction within zeolite crystals for selective formation of gasoline-ranged hydrocarbons. *J. Energy Chem.* 54, 429–433. doi:10.1016/j.jechem.2020.06.006

Wang, C., Zhai, P., Zhang, Z., Zhou, Y., Zhang, J., Zhang, H., et al. (2016). Nickel catalyst stabilization via graphene encapsulation for enhanced methanation reaction. *J. Catal.* 334, 42–51. doi:10.1016/j.jcat.2015.10.004

Wang, R., Chen, Y., Shang, X., Liang, B., Zhang, X., Zhuo, H., et al. (2024). Reversing the selectivity of alkanes and alkenes in iron-based fischer-tropsch synthesis: the precise control and fundamental role of sodium promotor. *ACS Catal.* 14, 11121–11130. doi:10.1021/acscatal.4c02252

Wang, Y., Zhao, Y., Liu, J., Li, Z., Waterhouse, G. I. N., Shi, R., et al. (2020). Manganese oxide modified nickel catalysts for photothermal CO hydrogenation to light olefins. *Adv. Energy Mater* 10, 1–9. doi:10.1002/aenm.201902860

Wind, T. L., Falsig, H., Sehested, J., Moses, P. G., and Nguyen, T. T. M. (2016). Comparison of mechanistic understanding and experiments for CO methanation over nickel. *J. Catal.* 342, 105–116. doi:10.1016/j.jcat.2016.07.014

Wolf, M., Fischer, N., and Claeys, M. (2020). Water-induced deactivation of cobalt-based Fischer–Tropsch catalysts. *Nat. Catal.* 3, 962–965. doi:10.1038/s41929-020-00534-5

Wolf, M., Fischer, N., and Claeys, M. (2021). Formation of metal-support compounds in cobalt-based Fischer-Tropsch synthesis: a review. *Chem. Catal.* 1, 1014–1041. doi:10.1016/j.checat.2021.08.002

Wu, W., Luo, J., Zhao, J., Wang, M., Luo, L., Hu, S., et al. (2024). Facet sensitivity of iron carbides in Fischer-Tropsch synthesis. *Nat. Commun.* 15, 6108–6111. doi:10.1038/s41467-024-50544-1

Xu, R., Hou, C., Xia, G., Sun, X., Li, M., Nie, H., et al. (2020). Effects of Ag promotion for Co/Al2O3 catalyst in Fischer-Tropsch synthesis. *Catal. Today* 342, 111–114. doi:10.1016/j.cattod.2019.04.004

Yahyazadeh, A., Borugadda, V. B., Dalai, A. K., and Zhang, L. (2022). Optimization of olefins' yield in Fischer-Tropsch synthesis using carbon nanotubes supported iron catalyst with potassium and molybdenum promoters. *Appl. Catal. A Gen.* 643, 118759. doi:10.1016/j.apcata.2022.118759

Yan, L., Liu, J., Wang, X., Ma, C., Zhang, C., Wang, H., et al. (2020). Ru catalysts supported by Si3N4 for Fischer-Tropsch synthesis. *Appl. Surf. Sci.* 526, 146631. doi:10.1016/j.apsusc.2020.146631

Zhai, P., Li, Y., Wang, M., Liu, J., Cao, Z., Zhang, J., et al. (2021). Development of direct conversion of syngas to unsaturated hydrocarbons based on Fischer-Tropsch route. *Chem* 7, 3027–3051. doi:10.1016/j.chempr.2021.08.019

Zhang, Y., Su, X., Li, L., Qi, H., Yang, C., Liu, W., et al. (2020a). Ru/TiO2 catalysts with size-dependent metal/support interaction for tunable reactivity in fischer–tropsch synthesis. *ACS Catal.* 10, 12967–12975. doi:10.1021/acscatal.0c02780

Zhang, Y., Yang, X., Yang, X., Duan, H., Qi, H., Su, Y., et al. (2020b). Tuning reactivity of Fischer–Tropsch synthesis by regulating TiOx overlayer over Ru/TiO2 nanocatalysts. *Nat. Commun.* 11, 3185. doi:10.1038/s41467-020-17044-4

Zhang, L., Zhang, J., Wang, G., Zhao, W., and Chen, J. (2022). Oxidation treatment of carbon aerogels supports to modulate Ru/CA catalysts for Fischer-Tropsch synthesis. *J. Fuel Chem. Technol.* 50, 1331–1340. doi:10.1016/S1872-5813(22)60031-8

Zhao, Y., Zhao, B., Liu, J., Chen, G., Gao, R., Yao, S., et al. (2016). Oxide-modified nickel photocatalysts for the production of hydrocarbons in visible light. *Angew. Chem.* 128, 4287–4291. doi:10.1002/ange.201511334

Zhou, Q.-L., and Zhou, Q.-L. (2016). Transition-metal catalysis and organocatalysis: where can progress Be expected? *Angew. Chem. Int. Ed.* 55, 5352–5353. doi:10.1002/ANIE.201509164